Anal Bioanal Chem (2017) 409:4071–4078
DOI 10.1007/s00216-017-0353-3

RESEARCH PAPER

In-situ hydrothermal synthesis of titanium dioxide nanorods on titanium wire for solid-phase microextraction of polycyclic aromatic hydrocarbons

Yu Tian[1] · Juanjuan Feng[1] · Yanan Bu[1] · Xiuqin Wang[1] · Chuannan Luo[1] · Min Sun[1]

Received: 31 January 2017 / Revised: 25 March 2017 / Accepted: 30 March 2017 / Published online: 17 April 2017

Abstract Titanium dioxide nanorods were prepared on the surface of titanium wire by hydrothermal synthesis for use as a solid-phase microextraction (SPME) fiber. The morphology of the SPME coating was observed by scanning electron microscopy (SEM). Employed in conjunction with gas chromatography (GC), the fiber was investigated with five polycyclic aromatic hydrocarbons (PAHs) and three terphenyls in direct-immersion extraction mode. Various parameters were optimized, such as the extraction time, the stirring rate, the extraction temperature, the ionic strength of the sample solution, and the desorption time. Under the optimized conditions, the SPME-GC analytical method achieved a low detection limit (0.003 μg L^{-1}) and wide linear ranges (0.01–100 μg L^{-1} and 0.01–200 μg L^{-1}) along with good correlation coefficients (0.9892–0.9962). The established method was also used to analyze rainwater and an aqueous solution of coal ash. The results indicated that this fiber could be applied in real-world environmental monitoring. The proposed fiber also exhibited excellent durability.

Keywords Titanium dioxide nanorods · Hydrothermal synthesis · Titanium wire · Solid-phase microextraction · Gas chromatography

✉ Min Sun
chm_sunm@ujn.edu.cn

[1] Key Laboratory of Chemical Sensing & Analysis in Universities of Shandong (University of Jinan), School of Chemistry and Chemical Engineering, University of Jinan, Jinan, Shandong 250022, China

Introduction

Solid-phase microextraction (SPME) as an efficient sample preparation technique that was introduced by Arthur and Pawliszyn in 1990 [1, 2]. It uses the adsorption of a stationary phase to extract analytes from a sample matrix; these analytes are then desorbed from the stationary phase and directed into an analytical instrument [3, 4]. SPME integrates sampling, preconcentration, extraction, and sample injection into one step, and can easily be coupled with gas chromatography (GC) and high-performance liquid chromatography (HPLC) [5]. Although solid-phase extraction (SPE) is the most popular method of extracting organics from aqueous samples, SPME has various advantages over SPE, such as a shorter extraction time, a smaller sample volume, solvent-free extraction, and higher enrichment efficiency. As it is a rapid, sensitive, and economical method [6], SPME has been widely applied in environmental testing [7], biological analysis [8], drug monitoring [9], and food testing [10]. However, commercial SPME fibers are costly and have some disadvantages, including low thermal and chemical stability, coating fragility, it is relatively easy to strip off the coating, and they have a tendency to expand in organic solvents [11]. The extraction coating is the most important factor in SPME, as it influences the extraction efficiency, stability, and applicability of this extraction technique. Therefore, the development of novel improved coatings is one of the most important ways to improve SPME technology.

The material used in the extraction coating is an important consideration because the extraction process is achieved through a distribution equilibrium between the sample solution and the extraction coating [12]. A series of materials have been explored as potential extraction coatings, such as metal nanometerials [13, 14], metal-organic frameworks [15, 16], organic polymers [14, 17], and molecularly imprinted

polymers [18, 19]. Nanomaterials have attracted particular attention in recent years and have been widely used in SPME technology [20]. These materials have unique surface structures and special properties that can enhance extraction efficiency and improve extraction selectivity [21].

Titanium dioxide (TiO_2) has been comprehensively studied and used in various fields. It is a very useful substance for preparing SPME coatings due to its chemical and thermal stability, biocompatibility, nonpolluting nature, low cost, and high corrosion resistance [22, 23]. There have been many studies on the use of TiO_2 in conjunction with nanowires, nanotubes, nanoparticles, and mesoporous materials [24–29]. Some studies have found that nanostructured TiO_2 is an excellent adsorbent for organic compounds when used in solid-phase extraction [30–32]. Liu et al. fabricated TiO_2 nanotube arrays on the surface of Ti wire for use in the SPME of polycyclic aromatic hydrocarbons (PAHs) [33]. Their results showed that TiO_2 nanotube arrays are capable of extracting PAHs, but the very thin nanotube walls make the coating very fragile and easy to destroy when carrying out SPME.

Inspired by the previous studies performed in this field, in the work reported in the present paper, we prepared a durable titanium dioxide nanorod coating with a high specific surface area on the surface of titanium wire for use in SPME. Hydrothermal synthesis was used to produce a uniform and tough titanium dioxide nanorod coating in situ, as this process is simple and easy to implement. PAHs are volatile nonpolar compounds that are produced during the incomplete combustion of organic matter such as coal, petroleum, wood, tobacco, and high-molecular-mass organic compounds. They are important environmental and food contaminants that are distributed globally [34]. We therefore applied the TiO_2-nanorod-coated Ti wire as an SPME fiber to extract PAHs from real-world samples (rainwater and an aqueous solution of coal) in order to check the extraction efficiency of the coated fiber. However, we also added some terphenyls to the samples to determine whether the coated fiber is effective at extracting nonpolar analytes too.

Experimental

Materials and reagents

The titanium wire (Φ 300 μm) was acquired from the Yixing Shenglong Metal Wire Net. Co. (Jiangsu, China). Anthracene (Ant), benzo[*a*]pyrene (BaP), chrysene (Chr), fluorene (Flu), fluoranthene (Fluor), *m*-terphenyl (*m*-TP), *o*-terphenyl (*o*-TP), and *p*-terphenyl (*p*-TP) were analytical grade and obtained from Shanghai Jingchun Industry Co. (Shanghai, China). Tetrabutyl titanate and KCl were both of analytical grade quality and purchased from Sinopharm Chemical Reagent Co. (Shanghai, China).

Apparatus

The detection and analysis of analytes were accomplished on a model 7890A GC system (Agilent Technologies, Palo, Alto, USA) equipped with a flame ionization detector (FID) and a split/splitless inlet. Chromatographic separation was achieved with a HP-5 capillary GC column (30 m × 0.32 mm i.d. × 0.25 μm film thickness; Agilent). Ultrapure nitrogen (>99.999%) was used as the carrier and make-up gases (flow rates: 3 mL min^{-1} and 25 mL min^{-1}, respectively). Splitless injection was performed at 300 °C. The detector temperature was set to 300 °C.

A scanning electron microscope (SEM; SUPRATM55, Carl Zeiss AG, Oberkochen, Germany) was used to characterize the surface morphology of the SPME fiber.

Preparation of the extraction coating

A similar titanium dioxide nanorod preparation method to that described in [35] was used in the present work. The first step was the preparation of the titanium dioxide seed layer. The titanium wire was cleaned sequentially with acetone, ethanol, and deionized water. It was immersed in a 0.5 mol L^{-1} ethanol solution of tetrabutyl titanate for 5 min and then dried by nitrogen. It was subsequently placed into a tube furnace and calcined at 350 °C for 30 min. This process was repeated three times, resulting in a titanium wire coated with a titanium dioxide seed layer.

The next step was to prepare the titanium dioxide nanorods. The titanium wire with a seed layer was transferred to a 100 mL high-pressure reaction kettle. A mixed solution containing 6 mL of hydrochloric acid (12 mol L^{-1}), 54 mL of ultrapure water, and 1 mL of tetrabutyl titanate was added to the reaction kettle. The reaction kettle was then sealed and placed in the oven at 180 °C for 7 h. The whole process was repeated three times, yielding titanium wire coated with titanium dioxide nanorods.

Sample preparation

A stock solution of five PAHs and three terphenyls containing Ant, BaP, Chr, Flu, Fluor, *m*-TP, *o*-TP, and *p*-TP at concentrations of 10 mg L^{-1} in ethanol was prepared and stored at 4 °C for use. Working solutions were prepared every day by diluting the stock solution to 20 μg L^{-1}. Rainwater and an aqueous solution of coal ash were collected and used as real-world samples. Rainwater was collected directly from the environment, filtered, and extracted directly. Coal ash was collected

from the boiler room of the University of Jinan. Ten grams of coal ash were extracted with 60 mL ethanol for about 6 h in a Soxhlet extractor. The extraction liquid was then concentrated to 20 mL and filtered, and 500 μL of the filtrate were added to a 250 mL solution for use as the aqueous solution of coal ash.

Solid-phase microextraction procedure

A homemade SPME device was refitted with a 5 μL syringe and equipped with the SPME fiber. The fiber was aged in the GC inlet at 300 °C for 5 min three times before performing any extraction. All extractions were performed by directly immersing the fiber in 10 mL of aqueous solution in a 15 mL flat tube. A magnetic bar was placed into the flat tube and set to spin at 1050 rpm to expedite the extraction, with the temperature maintained at 40 °C. After 30 min, the fiber was drawn back into the syringe and then interposed in the GC inlet at 300 °C to carry out thermal desorption for 5 min. After detection, the fiber was retained in the inlet for another 5 min to reduce possible carryover effects to a minimum. Each sample was extracted three times under the same extraction conditions, and detection was performed after each extraction simultaneously by GC/FID.

Results and discussion

Preparation of the extraction coating

Because of its hardness, good thermal stability, and chemical stability, using titanium wire as a support can increase the service life of a SPME fiber. Hydrothermal synthesis was used to prepare the TiO_2 coating. During the synthesis, using an excessively high acid concentration will corrode the titanium wire, but employing an acid concentration that is too low is not conducive to the formation of nanoparticles of a uniform size. Therefore, a suitable volume ratio of 6:54:1 hydrochloric acid (12 mol L^{-1}):ultrapure water:tetrabutyl titanate was adopted after some carrying out some tests. This volume ratio, as well as an optimized temperature of 180 °C and an optimized reaction time of 7 h, was adopted to promote the formation of a firm and uniform nanorod coating. The preparation process was repeated three times in order to obtain a thicker SPME coating.

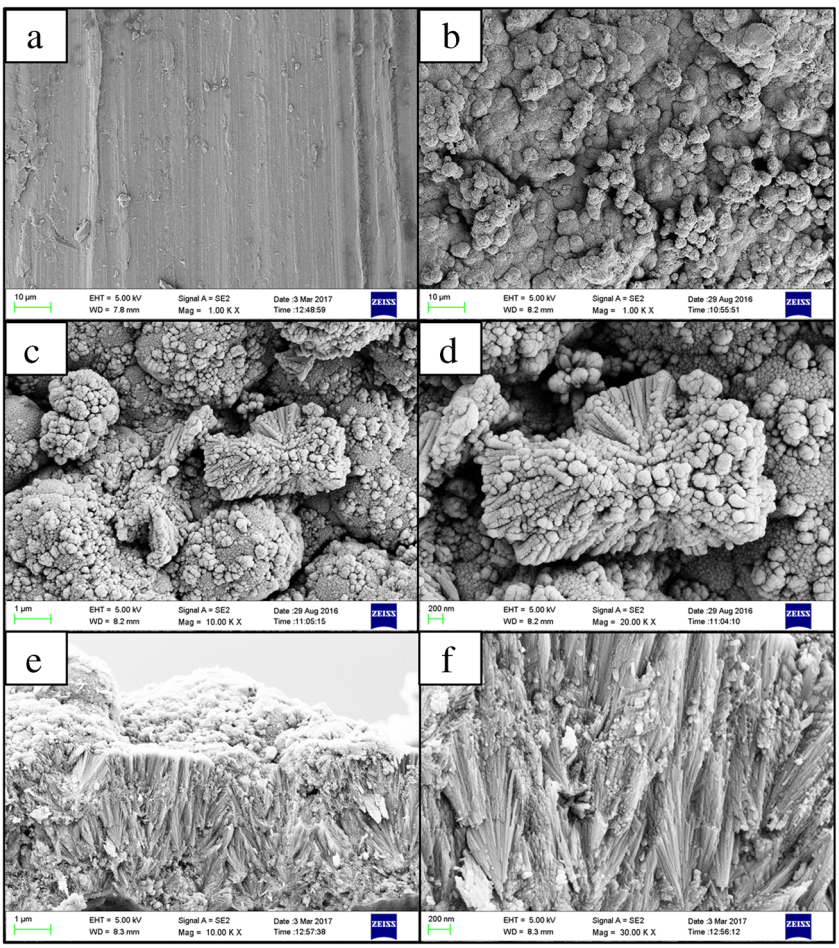

Fig. 1a–f SEM images of the smooth titanium wire and the coating of titanium dioxide nanorods on the SPME fiber obtained at different magnifications. **a** Smooth titanium wire. **b–d** Surface of the SPME fiber coating. **e–f** Cross-sections of the SPME fiber coating

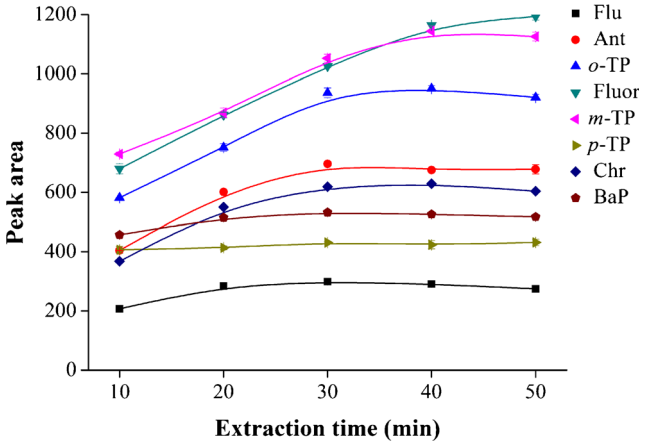

Fig. 2 Effect of the extraction time on the extraction efficiency. Conditions: extraction temperature, 40 °C; extraction time, 35 min; content of KCl, 20% (w/v); concentrations of the analytes, 20 μg L^{-1}; three extractions were performed at each extraction time

Characterization of the extraction coating

The surface morphologies of the titanium wire and the SPME fiber were characterized by SEM. Figure 1a clearly shows that the surface of the titanium wire is smooth. As seen in Fig. 1b, the microstructure of the coating is uniformly rough. In Fig. 1c–d, it is apparent that the coating includes 1–2 μm clusters of nanorods. As seen from the cross-section of the coating shown in Fig. 1e–f, the thickness of the coating is about 5–7 μm, and it is composed of multiple layers of nanorods (500–700 nm in length). There are some internal and external gaps in the nanorod clusters. This coating morphology greatly increases its surface area, improving mass transfer and extraction efficiency.

Optimization of the SPME conditions

The extraction conditions can strongly influence the extraction efficiency of the SPME fiber. In order to achieve the maximum extraction efficiency possible, the extraction conditions were optimized in a factor-by-factor optimization process that investigated the extraction time, stirring rate, extraction temperature, ionic strength of the sample solution, and desorption time.

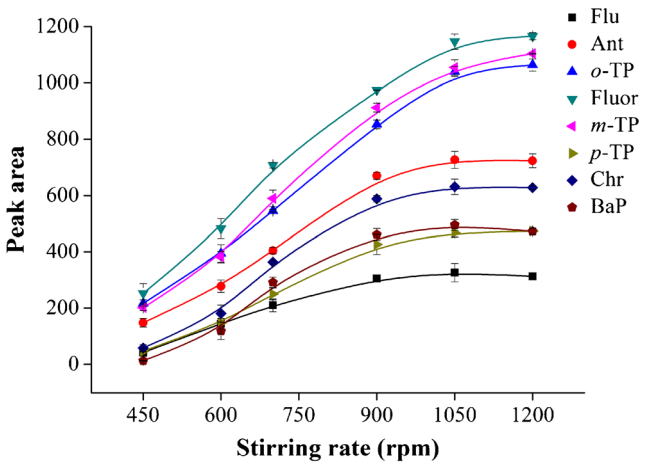

Fig. 3 Effect of the stirring rate on the extraction efficiency. Other conditions are the same as described in the caption for Fig. 2

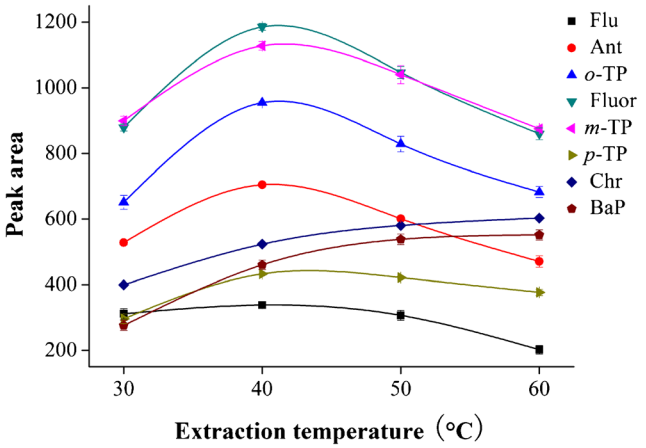

Fig. 4 Effect of the extraction temperature on extraction efficiency. Other conditions are the same as described in the caption for Fig. 2

Extraction time

SPME is an equilibrium-based extraction process, so the optimal extraction time should be the time taken for the system to reach equilibrium. The influence of the extraction time was studied by varying the extraction time from 10 to 50 min. As shown in Fig. 2, the peak areas of Flu, Ant, *o*-TP, and Chr steadily increase upon increasing the extraction time from 10 to 30 min, and then remain largely unchanged. The peak areas of *p*-TP and BaP do not change significantly regardless of the extraction time used, while the peak areas of *m*-TP and Fluor continueed to grow right up to the longest extraction time tested. However, the peak-area increases of Fluor and *m*-TP were

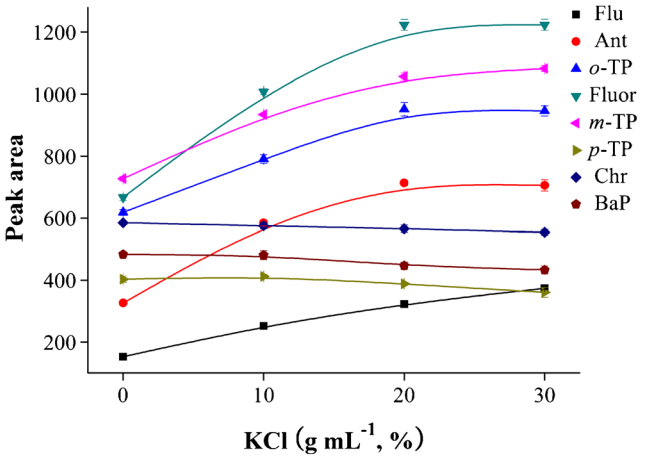

Fig. 5 Effect of the concentration of KCl (g mL^{-1}, %) on the extraction efficiency. Other conditions are the same as described in the caption for Fig. 2

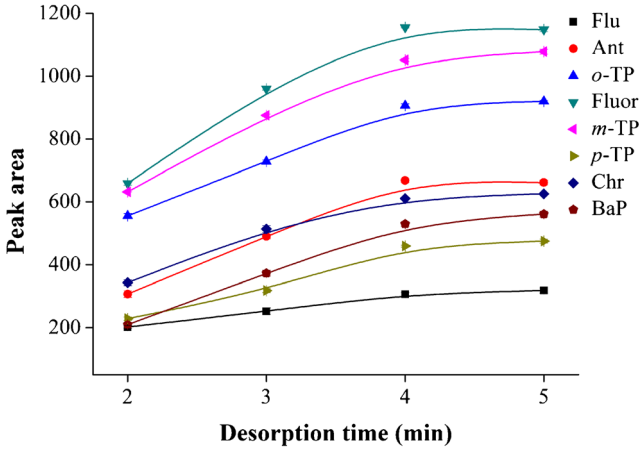

Fig. 6 Effect of the desorption time on the extraction efficiency. Other conditions are the same as described in the caption for Fig. 2

only 13.5 and 8.7% from 30 to 40 min, which are not significant. Considering the tradeoff between extraction efficiency and time taken to perform the extraction, 30 min was ultimately chosen as the optimal extraction time for subsequent studies. According to a previous report [33], the extraction time for a different SPME fiber coated with titanium dioxide nanotubes was 60 min, so the fiber created in the present work reduces the extraction time required considerably.

Stirring rate

Mass transfer is the molecular transfer process in the system due to uneven concentration. Increasing the stirring rate can effectively accelerate the mass transfer of the analytes to the extraction coating, and thus the extraction efficiency. However, a fast stirring rate will also produce vortices and bubbles in the solution, and it will increase mass-transfer resistance. The generation of vortices and bubbles causes air to enter the extraction interface, reducing the contact area of the SPME fiber with the solution, thereby hindering the mass-transfer process. The effect of the stirring rate on the extraction efficiency was investigated by increasing the stirring rate from 450 to 1200 rpm. As shown in Fig. 3, all of the peak areas increased up 1050 rpm but leveled off above that stirring rate. This means that the highest extraction efficiency for the analytes considered here was obtained at 1050 rpm, so this stirring rate was chosen for use in subsequent tests.

Extraction temperature

It is well known that increasing the temperature enhances the thermal motion of molecules. Therefore, increasing the temperature can significantly improve the extraction efficiency. However, the temperature also impacts on the partition coefficient of the target analytes between the fiber coating and the sample solution such that a high temperature may actually reduce the extraction efficiency. The effect of the temperature on the extraction efficiency was therefore studied by increasing the temperature from 30 to 60 °C. It can be seen from Fig. 4 that the peak areas of Flu, Ant, *o*-TP, Fluor, *m*-TP, and *p*-TP are highest when the temperature is 40 °C, while the peak areas of Chr and BaP increase slowly as the temperature rises from 40 to 60 °C. Therefore, 40 °C was chosen as the preferred extraction temperature for subsequent tests.

Ionic strength of the sample solution

Due to the formation of hydration spheres around ionic salt molecules, adding salt to an aqueous solution can reduce the solubility of organic analytes, thus increasing the concentrations of the organic analytes in the fiber coating. So, the effect of ionic strength was investigated by adding varying amounts of KCl to the working solutions and actual samples. As shown in Fig. 5, the peak areas of *p*-TP, Chr, and Bap show a slight downward trend with increasing ionic strength, while the peak areas of the other analytes first increased and then leveled off. Taking into account the balance between minimizing reagent costs and maximizing the extraction efficiency, a KCl content

Table 1 Analytical performance of the SPME-GC method

Analyte	Linear range (μg L^{-1})	[a] Correlation coefficient (*R*)	LOD (μg L^{-1})	[b] Repeatability ($n = 5$, RSD%) (single fiber)	[b] Repeatability ($n = 5$, RSD%) (fiber to fiber)
Flu	0.01–200	0.9959	0.004	1.94	2.02
Ant	0.01–200	0.9959	0.003	2.06	4.20
o-TP	0.01–100	0.9953	0.003	8.56	10.4
Fluor	0.01–200	0.9916	0.002	3.35	5.41
m-TP	0.01–200	0.9915	0.002	1.40	1.02
p-TP	0.01–200	0.9962	0.005	3.37	2.45
Chr	0.01–200	0.9892	0.004	1.35	2.14
BaP	0.01–100	0.9938	0.005	3.09	8.53

[a] Calibration level: $n = 9$

[b] Spiking level: 20 μg L^{-1}

Table 2 Recoveries of PAHs in the rainwater and the aqueous solution of coal ash, as obtained using the SPME-GC method developed in the present work

Analyte	Rainwater sample			Aqueous solution of coal ash		
	Concentration ($\mu g\ L^{-1}$, $n=3$)	[c]Recovery ($n=3$, RSD%)	[d]Recovery ($n=3$, RSD%)	Concentration ($\mu g\ L^{-1}$, $n=3$)	[c]Recovery ($n=3$, RSD%)	[d]Recovery ($n=3$, RSD%)
Flu	0.95 ± 0.03	109 ± 4.02	114 ± 3.84	5.10 ± 0.26	102 ± 7.43	92.4 ± 1.93
Ant	2.23 ± 0.12	85.8 ± 1.22	103 ± 1.43	2.91 ± 0.12	96.8 ± 4.21	105 ± 3.56
o-TP	1.21 ± 0.03	110 ± 2.53	109 ± 2.16	2.52 ± 0.09	88.1 ± 6.01	96.8 ± .62
Fluor	1.63 ± 0.07	108 ± 3.27	88.6 ± 3.01	3.06 ± 0.12	108 ± 4.51	113 ± 3.42
m-TP	[b] N.Q.	90.9 ± 6.64	98.5 ± 4.23	4.11 ± 0.21	94.5 ± 5.20	106 ± 1.51
p-TP	0.89 ± 0.01	98.2 ± 3.91	88.7 ± 1.94	[b] N.Q.	89.4 ± 2.51	92.4 ± 3.51
Chr	[a] N.D.	100 ± 2.67	93.4 ± 3.07	[b] N.Q.	109 ± 6.13	89.2 ± 3.08
BaP	2.79 ± 0.20	92.7 ± 6.43	104 ± 5.89	1.91 ± 0.04	116 ± 3.52	99.4 ± 6.06

[a] Not detected

[b] Detected but not quantified

[c] Spiking level: 10 $\mu g\ L^{-1}$. [d] Spiking level: 20 $\mu g\ L^{-1}$

of 20% (w/v) was ultimately chosen as the salt concentration for subsequent experiments.

Desorption time

Once adsorbed, the target analytes can then be desorbed completely by applying a sufficiently long desorption time. However, if the desorption time is too short, the analytes will not be desorbed completely, lowering the extraction efficiency. So the time above which the peak areas remain largely unchanged should be the best desorption time. In this study, the impact of desorption time on extraction efficiency was determined by increasing the desorption time from 2 to 5 min. In Fig. 6, the peak areas of all analytes are seen to increase consistently from 2 to 4 min, but when the desorption time is increased beyond 4 min, the peak areas remain largely unchanged. This indicates that the target analytes have been desorbed completely when the desorption time is 4 min, so this desorption time was ultimately chosen for use in subsequent studies.

Method evaluation

The analytical performance of the developed SPME-GC method for each analyte, including the linear range, the limit of detection (LOD), the correlation coefficient (R), and the extraction repeatability, is summarized in Table 1. These values were obtained under the optimized conditions by extracting from the standard working solutions. The curves obtained for Flu, Ant, Fluor, *m*-TP, *p*-TP, and Chr are linear in the range from 0.01 to 200 $\mu g\ L^{-1}$, and the curves for *o*-TP and BaP are linear from 0.01 to 100 $\mu g\ L^{-1}$. The curves also showed relatively high correlation coefficients of 0.9892–0.9962. The LODs (based on three times the signal-to-noise ratio) were studied by extracting from solutions of distilled water spiked with the analytes to various levels. The LODs

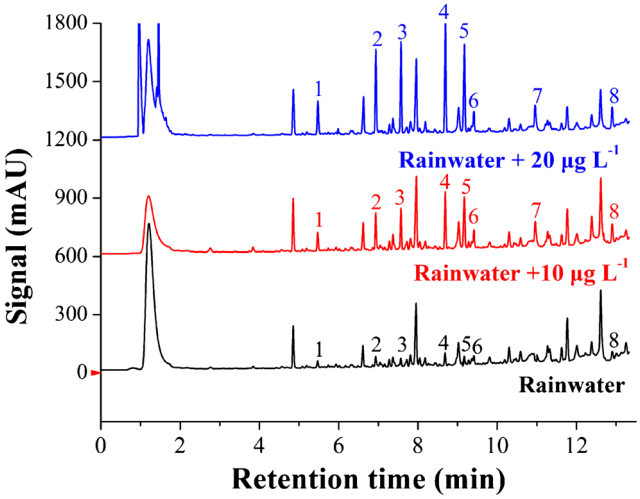

Fig. 7 GC chromatogram for the rainwater sample

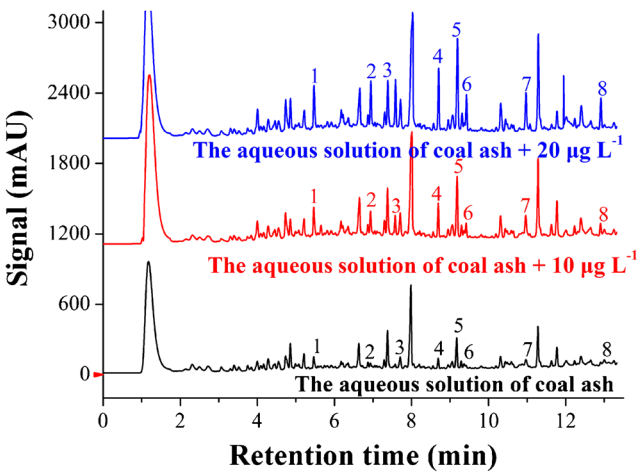

Fig. 8 GC chromatogram for the aqueous solution of coal ash

of the analytes were all 0.003 μg L^{-1}. The repeatability of one SPME fiber was determined by performing five successive extractions and then calculating the relative standard deviation; it was found to range from 1.35 to 8.56%. The fiber-to-fiber repeatability was also measured, and was found to range from 1.02 to 10.4%.

In order to evaluate the performance of the proposed SPME-GC method in the analysis of PAHs in real samples, rainwater and an aqueous solution of coal ash were extracted and analyzed using the method. The analytical results for the analytes in these real-world samples are summarized in Table 2. The concentrations of Flu, Ant, *o*-TP, Fluor, *p*-TP, Chr, and BaP in rainwater were 0.95, 2.23, 1.21, 1.63, 0.89, and 2.79 μg L^{-1}, respectively, and the standard deviations ranged from 0.03 to 0.20. *m*-TP was detected in rainwater but not quantified, while Chr was not detected. The concentrations of Flu, Ant, *o*-TP, Fluor, *m*-TP, and BaP in the aqueous solution of coal ash were 5.10, 2.91, 2.52, 3.06, 4.11, and 1.91 μg L^{-1}, respectively, and the standard deviations ranged from 0.04 to 0.26. *p*-TP as well as Chr were detected but were not quantified. The recoveries of the analytes spiked at 10 μg L^{-1} into the rainwater sample ranged from 85.8 to 110%, and they ranged from 88.6 to 114% when the spiking level was 20 μg L^{-1}. The relative standard deviations of those recoveries ranged from 1.22 to 6.64%. The recoveries of the PAHs spiked at 10 μg L^{-1} and 20 μg L^{-1} into the aqueous solution of coal ash were 88.1–116% and 89.2–113%. The relative standard deviations of those recoveries ranged from 1.51 to 7.43%. GC chromatograms for the actual samples are shown in Figs. 7 and 8. It is clear that the rainwater and the aqueous solution of coal ash were very rich in a wide range of organics.

Conclusions

A titanium wire was applied as a support to prepare a simple and useful SPME fiber. The wire was coated with TiO_2 nanorods through hydrothermal synthesis. The morphology of the coating was observed by SEM, and nanorod clusters were observed. When employed in conjunction with GC, the prepared fiber was applied to extract five PAHs and three terphenyls. The results indicated that the prepared fiber had high extraction efficiency, good mechanical strength, and excellent stability. The proposed SPME-GC method provided a low detection limit (0.003 μg L^{-1}), wide linear ranges (0.01–100 μg L^{-1} and 0.01–200 μg L^{-1}), and good correlation coefficients (0.9892–0.9962). The method was used to analyze a rainwater sample and an aqueous solution of coal ash, and it provided satisfactory results in that the recoveries of analytes were acceptable. The hydrothermal synthesis used in this work to coat the titanium wire is a simple technique, and the resulting nanorods in the coating showed a uniform particle size. The coating of TiO_2 nanorods generated in this work also presented excellent extraction performance. We intend to apply in situ hydrothermal synthesis to generate other nanomaterials for use as SPME coatings in subsequent studies.

Acknowledgements This work was supported by the National Natural Science Foundation of China (NSFC, nos. 21205048 and 21405061) and the Shandong Provincial Natural Science Foundation of China (no. ZR2014BQ019).

Compliance with ethical standards The authors declare that they have no conflict of interest.

References

1. Arthur CL, Pawliszyn J. Solid phase microextraction with thermal desorption using fused silica optical fibers. Anal Chem. 1990;62:2145–8.
2. Arthur CL, Killam LM, Buchholz KD, Pawliszyn J, Berg JR. Automation and optimization of solid-phase microextraction. Anal Chem. 1992;64:1960–6.
3. Chen J, Pawliszyn J. Solid phase microextraction coupled to high-performance liquid chromatography. Anal Chem. 1995;67:2530–3.
4. Zhang ZY, Yang MJ, Pawliszyn J, Solid-phase microextraction. A solvent-free alternative for sample preparation. Anal Chem. 1994;66:844A–53.
5. Guo M, Song W, Wang T, Li Y. Phenyl-functionalization of titanium dioxide-nanosheets coating fabricated on a titanium wire for selective solid-phase microextraction of polycyclic aromatic hydrocarbons from environment water samples. Talanta. 2015;144:998–1006.
6. Wardencki W, Curyło J, Namieśnik J. Trends in solventless sample preparation techniques for environmental analysis. J Biochem Bioph Methods. 2007;70:275–88.
7. Liu H, Liu L, Xiong Y, Yang X, Luan T. Simultaneous determination of UV filters and polycyclic musks in aqueous samples by solid-phase microextraction and gas chromatography-mass spectrometry. J Chromatogr A. 2010;1217:6747–53.
8. Zhang X, Cai JB, Oakes KD, Breton F, Servos MR, Pawliszyn J. Development of the space-resolved solid-phase microextraction technique and its application to biological matrices. Anal Chem. 2009;81:7349–56.
9. Kataoka H. Recent developments and applications of microextraction techniques in drug analysis. Anal Bioanal Chem. 2010;396:339–64.
10. Campillo N, Peñalver R, López-García I, Hernández-Córdoba M. Headspace solid-phase microextraction for the determination of volatile organic sulphur and selenium compounds in beers, wines and spirits using gas chromatography and atomic emission detection. J Chromatogr A. 2009;1216:6735–40.
11. Alpendurada MDF. Solid-phase microextraction: a promising technique for sample preparation in environmental analysis. J Chromatogr A. 2000;889:3–14.
12. Pawliszyn J. Solid-phase microextraction: theory and practice. New York: Wiley-VCH; 1997.
13. Zeng J, Zhao C, Chong F, Cao Y, Subhan F, Wang Q, et al. Oriented ZnO nanorods grown on a porous polyaniline film as a novel coating for solid-phase microextraction. J Chromatogr A. 2013;1319:21–6.
14. Wang T, Chen Y, Ma J, Qian Q, Jin Z, Zhang L, et al. Attapulgite nanoparticles-modified monolithic column for hydrophilic in-tube solid-phase microextraction of cyromazine and melamine. Anal Chem. 2016;88:1535–41.

15. Jia Y, Su H, Wang Z, Wong YE, Chen X, Wang M, et al. Metal–organic framework@microporous organic network as adsorbent for solid-phase microextraction. Anal Chem. 2016;88:9364–7.
16. Shih Y, Wang K, Singco B, Lin C, Huang H. Metal−organic framework−polymer composite as a highly efficient sorbent for sulfonamide adsorption and desorption: effect of coordinatively unsaturated metal site and topology. Langmuir. 2016;32:11465–73.
17. Chen L, Huang X. Sensitive monitoring of fluoroquinolones in milk and honey using multiple monolithic fiber solid-phase microextraction coupled to liquid chromatography tandem mass spectrometry. J Agric Food Chem. 2016;64:8684–93.
18. Patra S, Roy E, Madhuri R, Sharma PK. Fast and selective preconcentration of europium from wastewater and coal soil by graphene oxide/silane@Fe_3O_4 dendritic nanostructure. Environ Sci Technol. 2015;49:6117–26.
19. Roya M, Fatemeh K. Fabrication of ciprofloxacin molecular imprinted polymer coating on a stainless steel wire as a selective solid-phase microextraction fiber for sensitive determination of fluoroquinolones in biological fluids and tablet formulation using HPLC-UV detection. J Pharm Biomed Anal. 2016;122:98–109.
20. Pyrzynska K. Use of nanomaterials in sample preparation. TrAC Trends Anal Chem. 2013;43:100–8.
21. Sun M, Feng J, Qiu H, Fan L, Li X, Luo C. CNT–TiO_2 coating bonded onto stainless steel wire as a novel solid-phase microextraction fiber. Talanta. 2013;114:60–5.
22. Yang B, Uchida M, Kim HM, Zhan X, Kokubo T. Preparation of bioactive titanium metal via anodic oxidation treatment. Biomaterials. 2004;25:1003–10.
23. Liu X, Chu PK, Ding C. Surface modification of titanium, titanium alloys and related material for biomedical applications. Mater Sci Eng R. 2004;47:49–121.
24. Stankova NE, Dimitrov IG, Atanasov PA, Sakano T, Yata Y, Obara M. Proceedings of the EMRS 2009 Spring Meeting Symposium H: Synthesis, Processing and Characterization of Nanoscale Multi Functional Oxide Films II. Thin Solid Films. 2010;518:4597–602.
25. Kefi BB, El Atrache LL, Kochkar H, Ghorbel A. TiO_2 nanotubes as solid-phase extraction adsorbent for the determination of polycyclic aromatic hydrocarbons in environmental water samples. J Environ Sci. 2011;23:860–7.
26. Jiang L, Zhang W. Electrodeposition of TiO_2 nanoparticles on multiwalled carbon nanotube arrays for hydrogen peroxide sensing. Electroanal. 2009;21:988–93.
27. Mashhadizadeh MH, Afshar E. Electrochemical investigation of clozapine at TiO_2 nanoparticles modified carbon paste electrode and simultaneous adsorptive voltammetric determination of two antipsychotic drugs. Electrochim Acta. 2013;87:816–23.
28. Türker AR. Separation, preconcentration and speciation of metal ions by solid phase extraction. Sep Purif Rev. 2012;41:169–206.
29. Huang Y, Zhou Q, Xie G, Liu H, Lin H. Titanium dioxide nanotubes for solid phase extraction of benzoylurea insecticides in environmental water samples, and determination by high performance liquid chromatography with UV detection. Microchim Acta. 2011;172:109–15.
30. Pinkse MH, Uitto PM, Hilhorst MJ, Ooms B, Heck AJR. Selective isolation at the femtomole level of phosphopeptides from proteolytic digests using 2D-nanoLC-ESI-MS/MS and titanium oxide precolumns. Anal Chem. 2004;76:3935–43.
31. Chen C, Chen Y. Fe_3O_4/TiO_2 core/shell nanoparticles as affinity probes for the analysis of phosphopeptides using TiO_2 surface-assisted laser desorption/ionization mass spectrometry. Anal Chem. 2005;77:5912–9.
32. Zhou Q, Ding Y, Xiao J, Liu G, Guo X. Investigation of the feasibility of TiO_2 nanotubes for the enrichment of DDT and its metabolites at trace levels in environmental water samples. J Chromatogr A. 2007;1147:10–6.
33. Liu H, Wang D, Ji L, Li J, Liu S, Liu X, et al. A novel TiO_2 nanotube array/Ti wire incorporated solid-phase microextraction fiber with high strength, efficiency and selectivity. J Chromatogr A. 2010;1217:1898–903.
34. Li Q, Wang X, Chen X, Wang M, Zhao R. In situ hydrothermal growth of ytterbium-based metal–organic framework on stainless steel wire for solid-phase microextraction of polycyclic aromatic hydrocarbons from environmental samples. J Chromatogr A. 2015;1415:11–9.
35. Jiang S, Yi B, Zhang C, Liu S, Yu H, Shao Z. Vertically aligned carbon-coated titanium dioxide nanorod arrays on carbon paper with low platinum for proton exchange membrane fuel cells. J Power Sources. 2015;276:80–8.